

Dynamic Study of Poly(styrene-*vinyl-d*₃) in a Glassy Blend by Two-Dimensional Solid-State Deuteron NMR

Y. H. Chin, P. T. Inglefield,* and A. A. Jones

Department of Chemistry, Clark University, Worcester, Massachusetts 01610

Received April 2, 1993; Revised Manuscript Received July 2, 1993*

ABSTRACT: Reorientation of the polystyrene component in a compatible blend of polystyrene and poly(2,6-dimethylphenylene oxide) with 75% polystyrene was observed by two-dimensional solid-state deuteron NMR spectroscopy at the glass transition. A blend containing poly(styrene-*vinyl-d*₃) was studied as a function of temperature and mix time in the vicinity of the thermal glass transition. Chain motion of the deuterium-labeled polymer exhibited the characteristics of rotational Brownian diffusion with an associated broad distribution of correlation times. This distribution is considerably broader than that typical for single-component polymeric glasses and dynamically matches that previously observed for the chain motion of the other component in this particular blend. The dynamics of either component can only be simulated using a bimodal distribution, with each mode involving a distribution of correlation times. The relative weighting of the modes corresponded to local concentration fluctuations calculated using a statistical lattice model. This dynamic heterogeneity for both components in the blend is thus determined by the surroundings of the reference chain and not by the intrinsic dynamics of a given chain.

Introduction

Two-dimensional solid-state NMR has recently been applied to the investigation of reorientational motion in the vicinity of the glass transition.¹⁻⁶ This NMR experiment follows the motion at a very local level corresponding to the repeat unit. Since the time scale of the two-dimensional experiment is typically in the second to millisecond region which is comparable to time scales commonly employed in thermal, mechanical, and dielectric measurements, the repeat unit level motions detected by the NMR experiment can be directly linked in time and temperature to the bulk response of the polymer. The information available from the NMR experiment includes the rate of the motion, the geometry of the motion relative to the chemical structure of the repeat unit, the distribution of rates, and the temperature dependence of the rates. For the polymers investigated to date, the glass transition is associated with Brownian rotational diffusion, with a fairly broad distribution of rates extending over several decades.

Two of the studies of the glass transition have been carried out on multicomponent glasses:^{6,7} one a polymer/diluent glass and the other a polymer blend. In each of these cases only one component of the mixed glass was monitored and the purpose of this report is to characterize the dynamics of the second component in the polymer blend so that the motion of each component can be compared. The blend system under investigation is polystyrene (PS) and poly(phenylene oxide) (PXE), and the first two-dimensional NMR study⁶ monitored the motion of the PXE repeat units using the carbon-13 chemical shift anisotropy pattern from methyl carbon-13 labeled PXE. This study found the distribution of rates of Brownian rotational diffusion to be broader than that observed for single-component glasses. Also the carbon-13 two-dimensional patterns were best simulated by a bimodal distribution of correlation times for a 25% PXE blend. The weighting of the two modes was correlated with concentration fluctuations of the nearest neighbors which was estimated from a lattice model and an assumption of random mixing. Thus, for instance, the faster

relaxing mode for PXE units was associated with PXE surrounded by PS.

The glass transition temperature of PS is about 120 °C lower than PXE though a single glass transition temperature is observed in mechanical and thermal measurements.^{8,9} The glass transition is broader in the blends relative to the pure polymers, and this has been attributed to concentration fluctuations¹⁰ which is consistent with the interpretation presented for the NMR data. Recently, concentration fluctuations and the associated localized heterogeneities have been considered in a number of miscible polymer blends.¹¹⁻¹⁷ It should be emphasized that these heterogeneities are present in miscible blends which are intimately mixed even down to the repeat unit size scale, but, nevertheless, residual local heterogeneity remains. Fischer and Zetsche¹⁷ have characterized the concentration fluctuations by a Gaussian distribution, while the earlier two-dimensional NMR study used a lattice model,⁶ leading to a binomial distribution. This binomial distribution would go over to a Gaussian distribution in the continuum limit, corresponding to an increasing number of environments in the lattice model.

Other complications have been noted in the description of blend dynamics. The WLF equation appears to fail in such systems,¹³ which may be a reflection of the local concentration heterogeneity.¹⁵ Roland and Ngai¹⁶ relate changes in concentration fluctuations to changes in the extent of coupling. The primary coupling measure would be the effective width of the distribution of correlation times and the apparent activation energy.¹⁶ From the measurement of translational diffusion in polymer blends in another study,¹⁸ large positive deviations of the friction factor from the rule of additivity are noted as a function of concentration. Another factor contributing to observations of the temperature and composition dependence of motion at and above the glass transition may be the relative proximity of the lower critical solution temperature. If this temperature were close to the glass transition, larger concentration fluctuations might be encountered. A negative χ value has been determined from neutron scattering studies of the PXE/PS blend,¹⁹ though the exact nature of the thermodynamic interaction is a matter of continued study.^{20,21} This also could be expected to affect the concentration fluctuations.

* Abstract published in *Advance ACS Abstracts*, September 1, 1993.

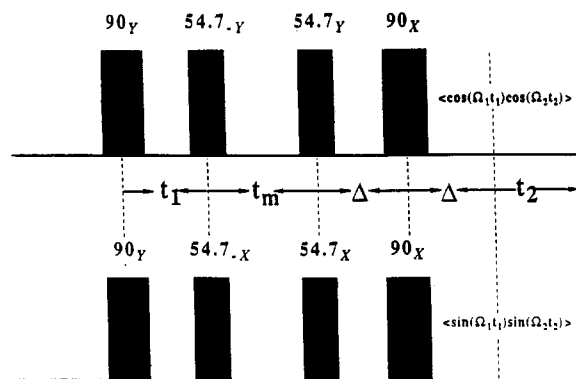


Figure 1. Two-dimensional pulse sequence for a deuterium exchange NMR experiment. Δ is the refocusing time.

The characterization of repeat unit level motion of the second component in the PXE/PS blend by solid-state NMR seems both timely and potentially useful in addressing a series of questions associated with blend dynamics. What is the relationship between the time scale and the distribution of rates for the two components? The information on hand on PXE could be compared with comparable data on PS by performing two-dimensional NMR experiments on PS-*d*₃ where only backbone hydrogens are replaced by deuterons. What are the relative temperature dependencies of the motions of the two components? In the earlier interpretation, only a distribution of correlation times corresponding to the stretched exponential was used. Would another form for the distribution alter the conclusions? Improvements have been made in the computer simulation of two-dimensional patterns so a more accurate interpretation of the earlier carbon-13 data is also possible. All of these points provide the motivation for the characterization of the local motional properties of PS in the PXE/PS blend by two-dimensional NMR.

Experimental Section

Sample preparation of the blend of poly(2,6-dimethylphenylene oxide) (PXE) and polystyrene (PS-*d*₃) is identical to the procedure described in the earlier NMR study.⁶ In this case, poly(styrene-*vinyl-d*₃) (ca. 98%) ($M_n = 27\,490$) purchased from Cambridge Isotope Laboratories was used to prepare a 25:75 PXE/PS-*d*₃ blend by weight. The glass transition temperature for 25:75 PXE/PS-*d*₃ previously measured by differential scanning calorimetry is 128 °C, and the new blend with PS-*d*₃ showed a single glass transition at the same temperature.

All experimental two-dimensional exchange ²H NMR spectra of chain deuterated polystyrene were obtained on Bruker MSL-300 NMR spectrometer, operating at a field of 7.05 T. This corresponds to a ²H resonance frequency of 46.07 MHz. A Bruker HP-300 BB (broad-band) probe with a probe-head comprising a coil of 5-mm diameter was used. The sample temperature was adjusted and maintained by introducing a steady flow of air (ca. 800 L/h) into the probe which was controlled by a Bruker VT-1000 heating unit in conjunction with a temperature sensor inserted inside the probe-head. A series of variable-temperature two-dimensional exchange experiments, ranging from 115 to 128 °C, were performed with different mixing times in the millisecond range.

The two-dimensional pulse sequence is depicted in Figure 1. The detailed description of the pulse techniques to obtain solid echo (real patterns) and spin alignment echo (imaginary patterns) has been presented elsewhere.²² In all cases, the phase cycling of each individual pulse involving 16 phases was employed to suppress unwanted artifacts. The durations of 90° and 54.7° pulses were 2.5 and 1.52 μ s, respectively. The lowest evolution time (t_1) was 0.8 μ s. The time interval between detection pulses was 20 μ s. The total spectral width was set to 312.5 kHz with 128 data points in the t_2 time domain and 64 data points in the

t_1 time domain, such that two complex time-domain data matrices of 64 \times 64 were acquired. Employing zero-filling in both dimensions, time-domain data matrices were extended to 128 \times 128 complex values. In all cases, the repetition time was set to 0.5 s.² This led to a total measurement time of between 2 and 3 days, depending upon the sample temperature.

All data processing of each time-domain data set was carried out on a VAX computer system employing the commercial software FTNMR. After appropriate Gaussian apodization, interpolation followed by extrapolation routines using a third-order polynomial were employed in both the t_1 and t_2 time domains to avoid phase twist caused primarily by time shift of the experimental data. In other words, both Fourier transformations with respect to rows and columns must start from $t_1 = t_2 = 0$ even though data acquisition starts at some later time. As a result, the cosine and sine data sets were scaled by different weighting factors prior to combination. The details of similar procedures for data processing have been described previously by Spiess et al.^{3,4} Multiplication of the first time domain data point by 0.5 is necessary to suppress t_1 glitches in both time dimensions prior to the application of Fourier transformation.

All experimental two-dimensional exchange ²H spectra with characteristic patterns, depending upon the duration of the different mixing times t_m , were interpreted by employing a simulation program on a VAX computer system. A 128 \times 128 matrix of simulated time domain signals was treated with the same data processing program (as used for experiment) to facilitate the comparison with experimental 2D data sets under consideration.

Results and Discussion

Experimental two-dimensional exchange ²H spectra for PS-*d*₃ in the 25:75 blend with mixing times of 1, 6, 12, 18, and 50 ms at 115 °C are presented in Figure 2. Similar data at 128 °C are shown in Figure 3. Data were obtained at three temperatures in the T_g region. Viewing these 2D patterns, it is evident that the experimental spectra gradually spread over the available plane of frequencies and develop a prominent square ridge of off-diagonal intensity with lengthening mixing time. In a 2D exchange experiment not only molecular reorientation but also spin diffusion can be detected. In practice, the spin diffusion between deuterons is inefficient and slow because of the relatively small dipolar coupling even when fully deuterated samples are used. Therefore, exchange signal patterns arising solely from molecular reorientation are to be expected especially at the rather short mix times (<50 ms) employed in this study. The broadening of the Pake pattern along the diagonal followed by the gradual spread of off-diagonal intensity over the whole available plane with lengthening mixing times indicates that chain motion can be ascribed to isotropic rotational diffusion by small-angle steps or Brownian diffusion.¹⁻³

The glass transition in pure PS-*d*₃ has been interpreted as isotropic rotational diffusion based on 2D patterns which were simulated using a distribution of correlation times covering 3 decades.³ Near the DSC T_g the average correlation time is on the order of seconds and rapidly diminishes to milliseconds when the temperature is raised 10 or 15 °C. In the data given in Figure 2 at 115 °C, a temperature some 10–15 °C below the thermal T_g , there is an observable off-diagonal intensity after mix times of a few milliseconds. This indicates the presence of rapid motion well below the thermal T_g in contrast to the case for pure PS or other single-component glasses³ but quite similar to the qualitative characteristics observed in this blend by monitoring motion of the PXE units using 2D carbon-13 patterns.⁶ On the other hand, at a temperature of 128 °C, the patterns in Figure 3 show both considerable off-diagonal intensity and the continued presence of a Pake type pattern along the diagonal. The presence of a

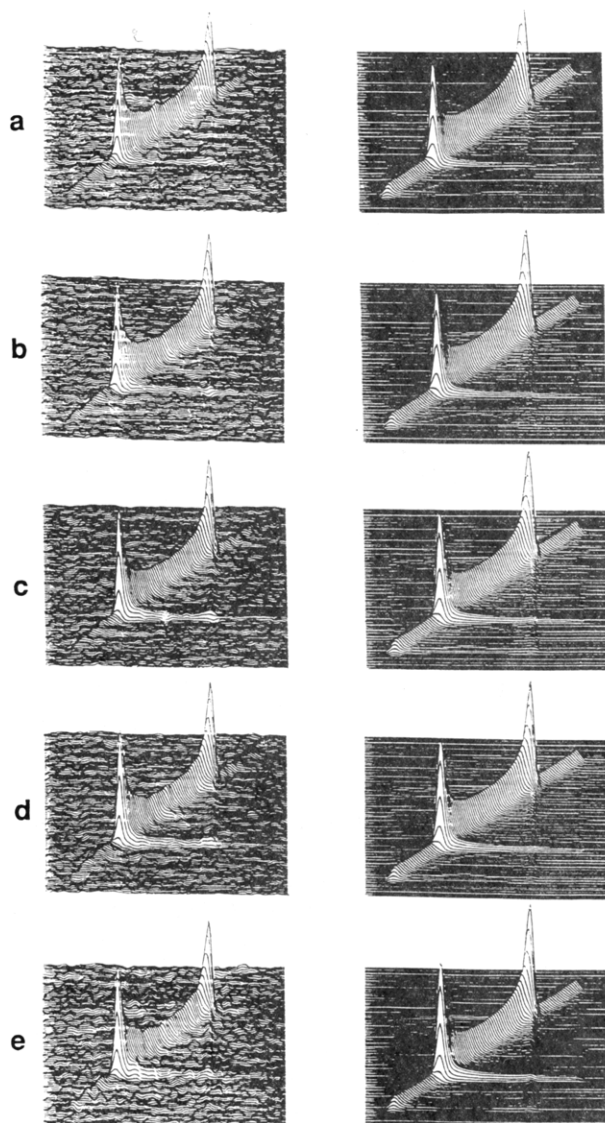


Figure 2. Two-dimensional ^2H exchange patterns for PS- d_3 in the 25:75 blend as a function of mixing time at 115 °C: (a) 1, (b) 6, (c) 12, (d) 18, and (e) 50 ms. Experimental patterns on the left are compared with simulated 2D patterns on the right.

significant amount of intensity along the diagonal indicates the presence of slowly reorientating units at this temperature well above the thermal T_g . The presence of rapidly relaxing units well below T_g and of slowly relaxing units well above T_g indicates the presence of a very broad distribution of relaxation times relative to that observed on single-component glasses. This behavior is at least qualitatively reminiscent of the patterns observed by carbon-13 on the PXE in this same blend.⁶

To quantitatively interpret the 2D patterns, two distributions of correlation times have been used. The interpretation of motion in pure PS is based on a log Gaussian distribution.³ This correlation function is typically expressed as

$$\phi(t) = \frac{1}{\sigma(2\pi)^{1/2}} \exp\left\{-\frac{\ln(t_m/\tau_c)^2}{2\sigma^2}\right\} \quad (1)$$

where the ratio $\ln(t_m/\tau_c)$ determines the time scale of the motion and the standard deviation σ controls the width of the distribution. For this symmetric distribution, τ_c is the mean correlation time and t_m is the mixing time. The second distribution which has been employed corresponds to the stretched exponential correlation function given by

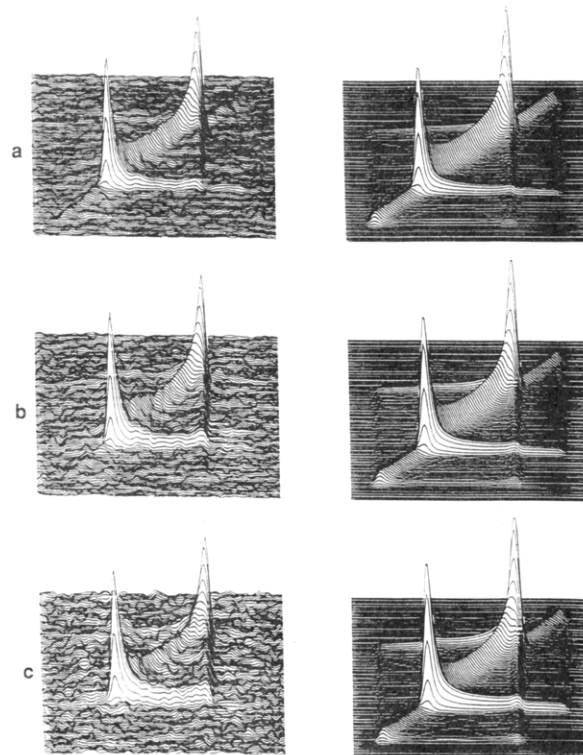


Figure 3. Two-dimensional ^2H exchange patterns for PS- d_3 in the 25:75 blend as a function of mixing time at 128 °C: (a) 6, (b) 18, and (c) 50 ms. Experimental patterns on the left are compared with simulated 2D patterns on the right.

the expression

$$\phi(t) = \exp(-(t_m/\tau_p)^\alpha) \quad (2)$$

where the breadth of the distribution is controlled by the exponent α and the time scale by the characteristic correlation time τ_p . In practice, the stretched exponential correlation function is written as a weighted sum of exponential correlation functions as described elsewhere.^{6,26} For either distribution, the time-domain response corresponding to each exponential correlation time is calculated following the procedures developed by Spiess et al.^{2,3} and then summed to give the response corresponding to the distribution. As mentioned earlier this theoretical time-domain response is treated with the same data handling procedures as the experimentally acquired time-domain information. This differs from the earlier treatment of the carbon-13 data⁶ which were simulated in the frequency domain, so the carbon-13 patterns⁶ will be resimulated in this report in order to treat deuterium patterns and the carbon-13 patterns in an identical manner. An additional improvement in the interpretation is also made by considering the possibility of motion during the evolution and detection periods.³ With motions on the time scale of milliseconds, only a few percent of the intensity is lost in the deuterium patterns but the correction will be applied to both the carbon and deuterium simulations.

If a reinterpretation of the carbon-13 data is undertaken first, the general situation is quite similar to the earlier report.⁶ Neither a single-exponential correlation time nor a distribution corresponding to a single stretched exponential is capable of matching the observed 2D patterns as a function of mix time. As before, a bimodal distribution of correlation times corresponding to two stretched exponentials is required to match the PXE dynamics in the 25:75 (PXE/PS) blend data. Experimental and simulated patterns are given in Figure 4, and the param-

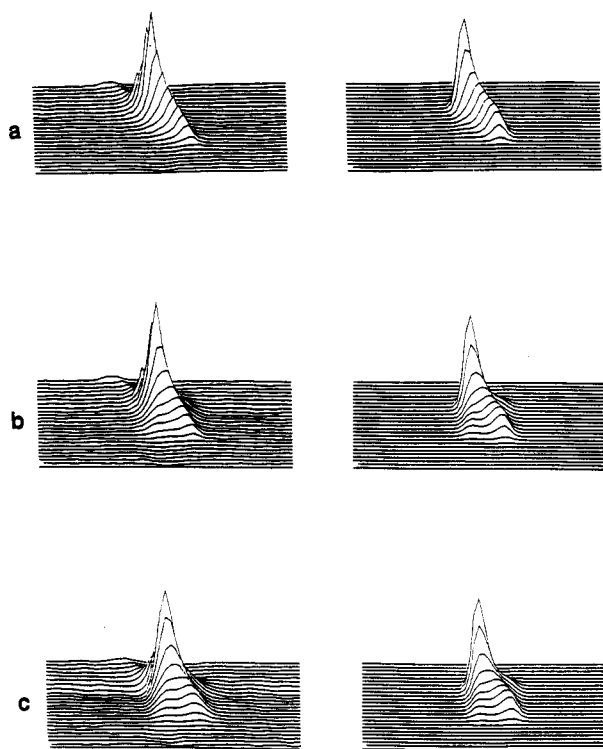


Figure 4. Two-dimensional ^{13}C exchange patterns for the PXE in a 25:75 blend as a function of mixing time at 115 °C: (a) 1, (b) 50, and (c) 100 ms. Experimental patterns on the left are compared with the improved 2D simulated patterns on the right.

Table I. Simulation Parameters for the Dynamics of the PXE Chain in the PXE/PS (25:75) Blend Using the Stretched Exponential Distribution Function

temp (°C)	115	120	128
α	0.4	0.3	0.3
τ_p (75% slow component) (s)	3.0	0.65	0.25
α	0.8	0.8	0.8
τ_p (25% fast component) (ms)	10	5	5

Table II. Simulation Parameters for the Dynamics of the PXE Chain in the PXE/PS (50:50) Blend Using the Stretched Exponential Distribution Function

temp (°C)	150	157
α	0.99	0.99
τ_p (10% rigid component) (s)	10	10
α	0.3	0.3
τ_p (80% slow component) (s)	2.0	0.2
α	0.8	0.8
τ_p (10% fast component) (ms)	10	5

eters of the simulation are given in Table I. The interpretation of the 50:50 blend again involves the same general type of distribution as reported before.⁶ At this concentration two stretched exponentials are employed plus a rigid component which is added at an arbitrary correlation time which is slow relative to the mix times.

The improved interpretation of the 25:75 carbon-13 data on PXE does not change the relative weighting of the two stretched exponentials. The fast component corresponds to 25% of the intensity, while the slow component corresponds to the remaining 75%. The fractional exponents of the two distributions are a little broader than in the earlier interpretation, while the characteristic correlation times have become slower. The 50:50 carbon-13 interpretation changes in a similar manner relative to the earlier version, and the new simulation parameters are reported in Table II. The interpretation of the carbon-13 patterns given here is felt to be more accurate because experiment and simulation were handled in the same manner after their respective generation in the time

domain. The identical apodization of both experiment and simulation is the most important feature in the improvement.

The interpretation of the 2D deuterium patterns on the 25:75 blend began with a single-exponential correlation function and proceeded to a single stretched exponential correlation function. However, both of these approaches are unable to match the development of the patterns as a function of mix time. This outcome parallels the qualitative differences seen for multicomponent glasses relative to single-component glasses. As with the carbon-13 data on PXE, the deuterium data on PS- d_3 in the 25:75 blend can be simulated with a distribution corresponding to two stretched exponential correlation functions as shown in Figures 2 and 3. The slower relaxing component corresponds to 75% of the intensity just as it did with the carbon-13 interpretation. The characteristic relaxation times and exponents for the patterns at all three temperatures are given in Table III. The plots of the distributions of exponential correlation times are displayed in Figure 5.

To check for any dependence on the choice of distribution function, the interpretation of the deuterium data was repeated using the log Gaussian distribution function. A single log Gaussian distribution is no more successful than a single stretched exponential correlation function, and two log Gaussian distributions must be combined to match the patterns as a function of mix time. The weighting of the two log Gaussian distributions is the same as for the case of the stretched exponential function with the slow component associated with 75% of the intensity. The log Gaussian distributions employed to interpret the data at all three temperatures are shown in Figure 6 along with the stretched exponential distributions. In general, the two types of distributions are quite similar. The asymmetric stretched exponential distributions have slightly different widths and time scales, but the overall nature of the two types of distributions is much the same. Thus the need to resort to a bimodal distribution exists and the relative weightings of the modes of the distribution are not strongly dependent on the choice of the particular mathematical form used for the modes.

The need to invoke a bimodal distribution can be understood by considering the probability, $P(\theta)$, of finding a molecule at orientation θ given that, at time zero, θ is zero. This probability, calculated from the correlation functions of the interpretations, is plotted for the fast and slow components of the distribution in Figure 7. At all three temperatures, the slow component remains localized near a 0 of zero while the fast component is spread over all angles with nearly equal probability. A monomodal distribution is unlikely to match this characteristic, which is a common feature present in the patterns to be interpreted.

The primary purpose of this study is to compare the local motion of the PS component with that of the PXE component at a specific temperature and composition. We are now in a position to compare the distribution of correlation times obtained by interpreting the carbon-13 patterns from labeled PXE with the distribution of correlation times obtained from the deuterium patterns of PS- d_3 for the 25:75 blend. These are shown in Figure 8 for all three temperatures studied. There is a remarkable coincidence between the dynamics seen from the two different polymer backbones in terms of time scale, breadth of distribution, and relative weighting of the modes.

To understand this coincidence, we will refer to the lattice model initially invoked in a discussion of the relative

Table III. Simulation Parameters for the Dynamics of the PS Chain in the PXE/PS (25:75) Blend

log Gaussian distribution				stretched exponential distribution			
temp (°C)	115	120	128	temp (°C)	115	120	128
σ	4.0	4.0	3.5	α	0.3	0.3	0.25
τ_c (75% slow component) (s)	2	0.5	0.1	τ_p (75% slow component) (s)	6	1.25	0.25
σ	1.5	1.5	1.5	α	0.8	0.8	0.8
τ_c (25% fast component) (ms)	1.5	1	1	τ_p (25% fast component) (s)	1.5	1	1

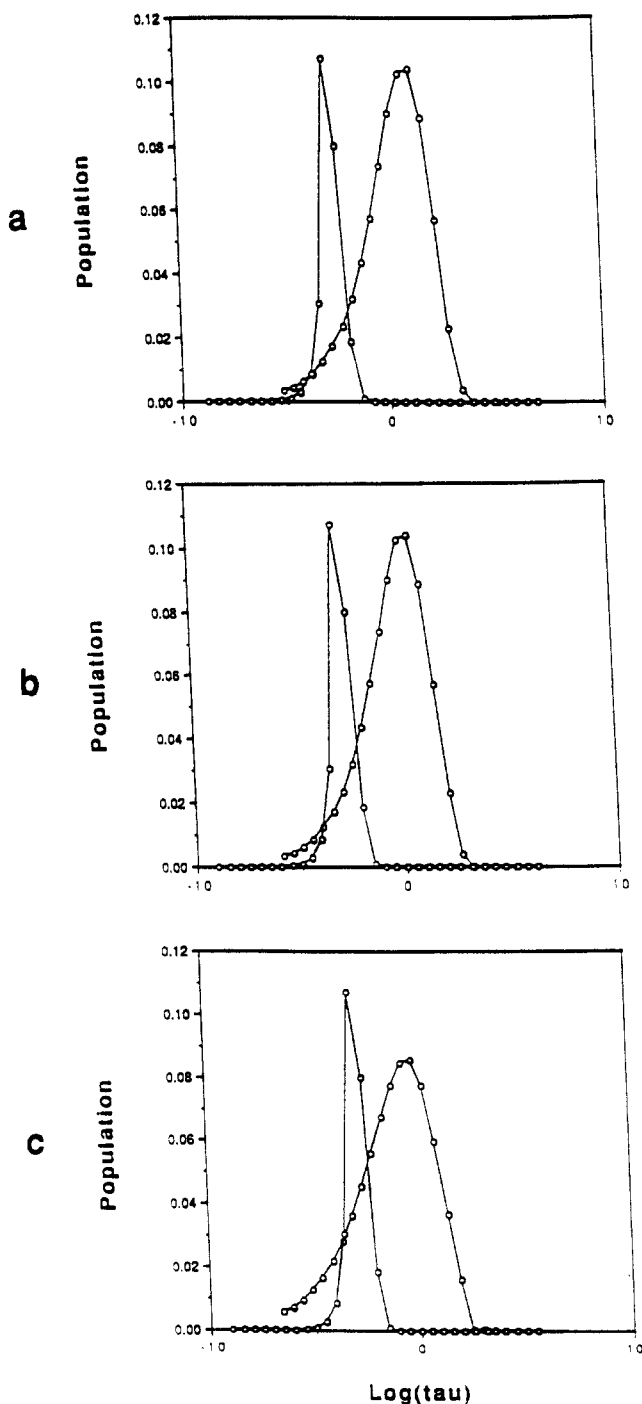


Figure 5. Distribution of exponential correlation times for the PS- d_3 component in 25:75 blends at temperatures of (a) 115, (b) 120, and (c) 128 °C.

weighting of the modes of distributions of correlation times in multicomponent glasses.^{6,21,23-25} The lattice model is used to count nearest-neighbor contacts where lattice sites are occupied by either PS or PXE units. In this development, the mobility of the nearest neighbors is considered to affect the relative mobility of the reference unit under consideration. Thus, if the mobilities of the PS units are considered, the most mobile PS units will be those

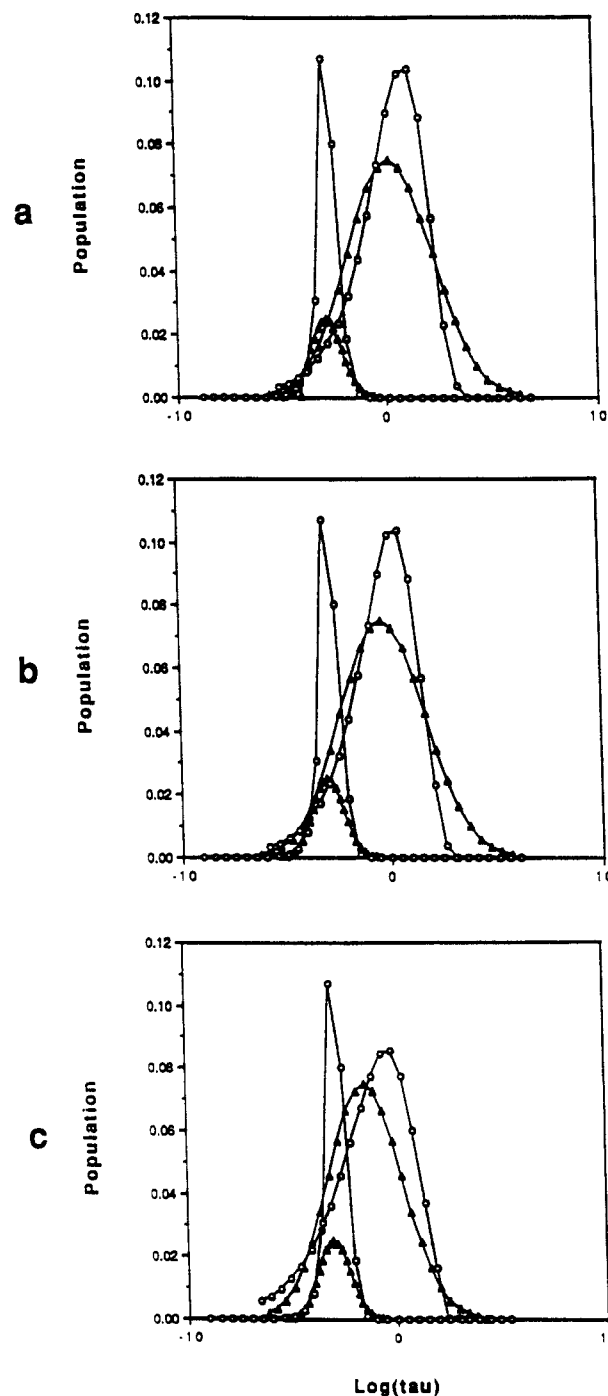


Figure 6. Log Gaussian distributions of correlations, indicated by the symbol Δ , superimposed with the stretched exponential distribution of correlation times, indicated by the symbol O for the PS component in 25:75 blends at temperatures of (a) 115, (b) 120, and (c) 128 °C. The comparison between the mean correlation time with the width of distribution and the characteristic time with fractional exponents is given in Table III.

surrounded by other PS units since this is the lower T_g material. Likewise, the most mobile PXE units will be surrounded by PS units. To make up the lattice for this blend, 3 PS repeat units are considered to occupy the same number of lattice sites as 2 PXE repeat units: a ratio

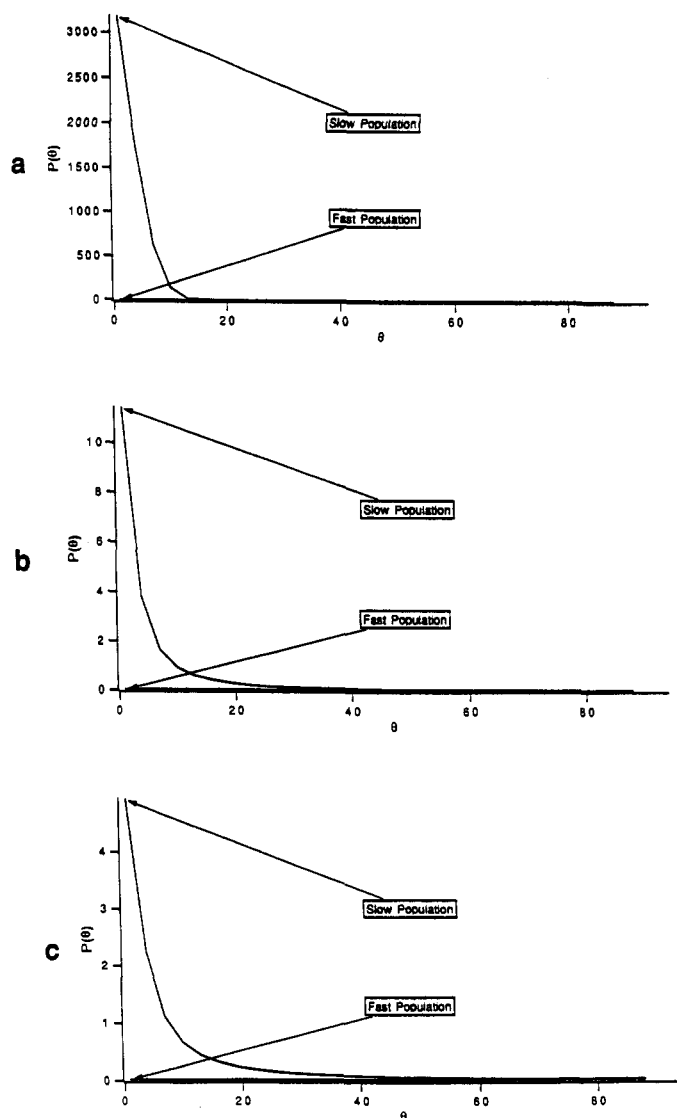


Figure 7. Probability of finding an orientational angle θ at a time t based on the simulated 2D patterns for PS- d_3 in the 25:75 blend at a mix time of 50 ms and at temperatures of (a) 115, (b) 120, and (c) 128 °C.

determined from a molecular modeling calculation on the two chains.^{6,21} To calculate nearest-neighbor contacts, the quantity F_j is defined, which is the fraction of PS which have j PXE units as nearest neighbors on the lattice. The F_j 's can be written in terms of the fraction of lattice sites, d , occupied by PS units and the fraction of lattice sites occupied by PXE units, $p = 1 - d$. For the 25:75 composition, $p = 0.3$ and

$$\begin{aligned} F_0 &= d^4 = 0.24 \\ F_1 &= 4d^3p = 0.41 \\ F_2 &= 6d^2p^2 = 0.265 \\ F_3 &= 4dp^3 = 0.076 \\ F_4 &= p^4 = 0.008 \end{aligned} \quad (3)$$

Thus the fraction of most mobile PS units is 0.24 which is in close agreement with the value of 0.25 determined from simulating the deuterium 2D patterns. The 75% slow component would be associated with a sum of the remaining nearest-neighbor environments which all contain the less mobile PXE units. Exactly the same equations apply if the reference unit is thought to be PXE so that the lattice model again predicts 24% of the PXE

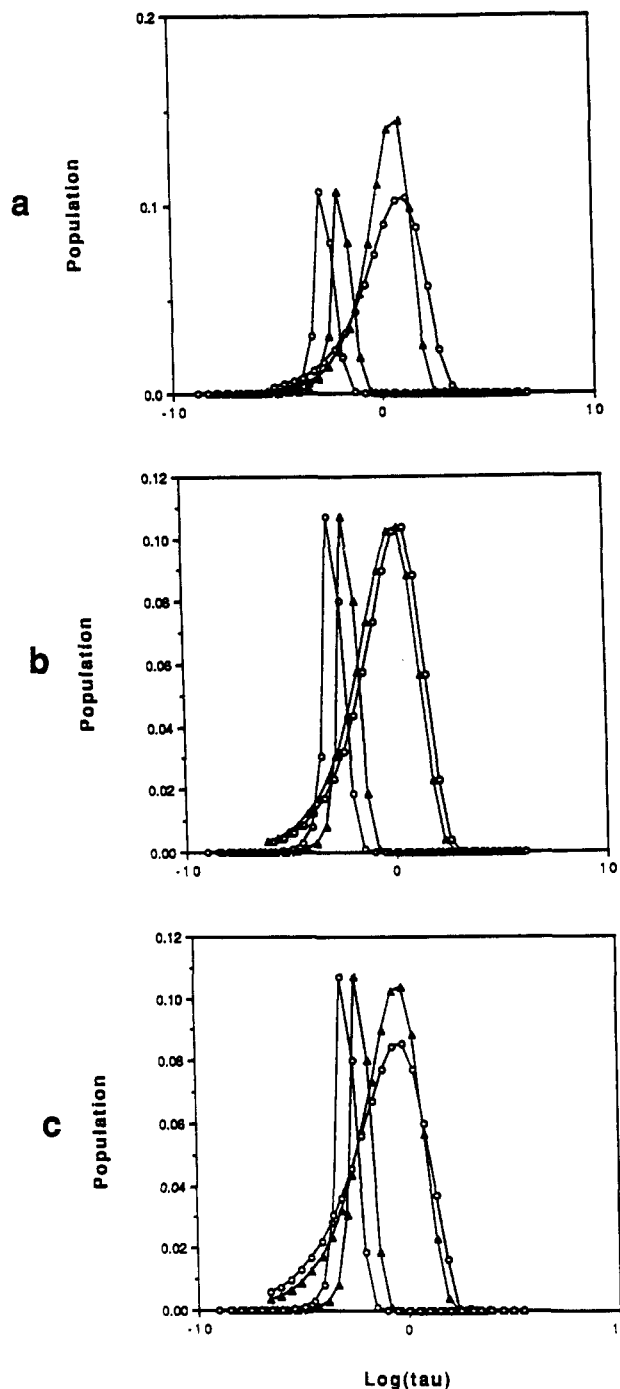


Figure 8. Combined stretched exponential distribution of correlation times for 25% diluent PXE- $^{13}\text{CH}_3$, indicated by the symbol Δ , superimposed with that for 75% PS- d_3 in a blend indicated by the symbol \circ .

units are surrounded by PS units and would therefore have the highest mobility. The experimental result determined from the simulation of the carbon-13 data on labeled PXE places the fast population at 25%, thus once more closely matching the lattice model result. The lattice model, nearest-neighbor argument also explains why the fast population (0.24) is the same whether the dynamics of PS or PXE is considered as long as the blend composition is held constant.

Carbon-13 data on PXE in the 50:50 blend were also acquired,⁶ and three components were required to simulate the observed patterns. The experimental results are 10% rigid, 80% slow, and 10% fast. The rigid component is a reference unit surrounded completely by PXE units which is a negligible fraction according to the lattice model for the 25:75 blend, but for the 50:50 blend this increases

to 10% experimentally, matching the simulation estimates at both concentrations. In particular, at the 50:50 composition the lattice model predicts the slow component to be 86% and the fast component to be 4%. Given a likely error of 5% in the simulation of the patterns, experimental and predicted weightings are again in satisfactory agreement.

Conclusions

The concentration fluctuation estimates from the lattice model appear to provide a basis to understand the distributions of correlation times employed to simulate the 2D patterns. Thus, while the glass transition dynamics of the two components have merged to a narrow range of temperatures relative to the differences in glass transition temperature of the constituents as pure polymers, residual heterogeneities persist. These heterogeneities are produced by the surroundings not by the intrinsic dynamics of the reference unit. Thus PXE repeat units surrounded by PS units move much like PS units surrounded by PS units. This agrees with the picture presented by Ngai and Roland on the importance of the coupling parameters in the dynamical heterogeneity of miscible polymer blends.¹⁶ In recent dielectric studies, the increase in breadth of the relaxation times can be seen,^{11,17} but NMR is particularly adept at tracking the motion of both components in the blend independently which allowed for the identification of the importance of the surroundings relative to the role of the reference chain unit. The PXE units surrounded by PS units do appear to move somewhat slower than PS units surrounded by PS units as can be seen in Figure 8. This would be expected based on the relative time scales of motion for the individual isolated polymer chains as would be observed in solution,^{27,28} but it is the intermolecular factors which dominate the multimodal nature of the distribution of correlation times in the glass.

Acknowledgment. Support from Office of Naval Research Grant N00014-90-J-1006 is greatly appreciated. The authors thank Dr. Dieter Schaefer for valuable discussions about the simulation program and the deuteron 2D exchange experiments. We are grateful to Mr. Changan Zhang for providing the useful software needed to process the experimental 2D data.

References and Notes

- (1) Wefing, S.; Spiess, H. W. *J. Chem. Phys.* **1988**, *89*, 1219.
- (2) Wefing, S.; Kaufmann, S.; Spiess, H. W. *J. Chem. Phys.* **1988**, *89*, 1234.
- (3) Kaufmann, S.; Wefing, S.; Schaefer, D.; Spiess, H. W. *Macromolecules* **1990**, *23*, 3431.
- (4) Schaefer, D.; Spiess, H. W.; Suter, U. W.; Fleming, W. *Macromolecules* **1990**, *23*, 3431.
- (5) Zemke, K.; Chmelka, B. F.; Schmidt-Rohr, K.; Spiess, H. W. *Macromolecules* **1991**, *24*, 6906.
- (6) (a) Chin, Y. H.; Zhang, C.; Wang, P.; Jones, A. A.; Inglefield, P. T. *Macromolecules* **1992**, *25*, 3031.
- (7) Zhang, C.; Wang, P.; Jones, A. A.; Inglefield, P. T. *Macromolecules* **1991**, *24*, 338.
- (8) Yee, A. F. *Polym. Eng. Sci.* **1977**, *17*, 213.
- (9) Stoelting, J.; Karasz, F. E.; MacKnight, W. J. *Polym. Eng. Sci.* **1970**, *10*, 133.
- (10) MacKnight, W. J.; Stoelting, J.; Karasz, F. E. *Adv. Chem. Ser.* **1971**, *99*, 29.
- (11) Keskkula, H.; Paul, D. R.; Young, P.; Stein, R. S. *J. Appl. Polym. Sci.* **1987**, *34*, 1861.
- (12) Ngai, K. L.; Roland, C. M.; O'Reilly, J. M.; Sedita, J. S. *Macromolecules* **1992**, *25*, 3906.
- (13) O'Reilly, J. M.; Sedita, J. S. *Mater. Res. Soc. Symp. Proc.* **1990**, *171*, 225.
- (14) Colby, R. H. *Polymer* **1989**, *30*, 1275.
- (15) Miller, J. B.; McGrath, K. J.; Roland, C. M.; Trask, C. A.; Garroway, A. N. *Macromolecules* **1990**, *23*, 4543.
- (16) Roland, C. M.; Ngai, K. L. *Macromolecules* **1991**, *24*, 2261.
- (17) Fischer, E. W.; Zetsche, A. *Polym. Prepr. (Am. Chem. Soc., Div. Polym. Chem.)* **1992**, *33* (1), 78.
- (18) Green, P. F.; Adolf, D. B.; Gilliom, L. R. *Macromolecules* **1991**, *24*, 3377.
- (19) Maconnachie, A.; Kambour, R. P.; White, D. M.; Rostami, S.; Walsh, D. J. *Macromolecules* **1987**, *17*, 2645.
- (20) Aurelio de Araujo, M.; Oelfin, D.; Stadler, R.; Moeller, M. *Makromol. Chem., Rapid Commun.* **1989**, *10*, 259.
- (21) Wang, P.; Jones, A. A.; Inglefield, P. T.; White, D. M.; Bendler, J. T. *New Polym. Mater.* **1990**, *2*, 221.
- (22) Schmidt, C.; Blumich, B.; Spiess, H. W. *J. Magn. Reson.* **1988**, *79*, 269.
- (23) Cauley, B. J.; Cipriana, C.; Ellis, K.; Roy, A. K.; Jones, A. A.; Inglefield, P. T.; McKinley, B. J.; Kambour, R. P. *Macromolecules* **1991**, *24*, 403.
- (24) Liu, Y.; Roy, A. K.; Jones, A. A.; Inglefield, P. T.; Ogden, P. *Macromolecules* **1990**, *23*, 968.
- (25) Jones, A. A.; Inglefield, P. T.; Liu, Y.; Roy, A. K.; Cauley, B. J. *J. Non-Cryst. Solids* **1991**, *131*, 556.
- (26) Roy, A. K.; Jones, A. A.; Inglefield, P. T. *Macromolecules* **1986**, *19*, 1356.
- (27) Jones, A. A.; Lubianez, R. P. *Macromolecules* **1978**, *11*, 126.
- (28) Matsuo, K.; Kuhlmann, K. F.; Yang, H. W.-H.; Geny, F.; Stockmayer, W. H.; Jones, A. A. *J. Polym. Sci. Polym. Phys. Ed.* **1977**, *15*, 1347.